

Title: Intracranial functional haemodynamic relationships in patients with cerebral small vessel disease

Authors: Gordon W Blair^{1,2}
Michael J Thrippleton^{1,2}
Yulu Shi^{1,2,3}
Iona Hamilton^{1,2}
Michael Stringer^{1,2}
Francesca Chappell¹
David Alexander Dickie⁴
Peter Andrews¹
Ian Marshall¹
Fergus N Doubal^{1,2}
Joanna M Wardlaw^{1,2,5}

¹Brain Research Imaging Centre, Centre for Clinical Brain Sciences, University of Edinburgh, Edinburgh, UK

²UK Dementia Research Institute at The University of Edinburgh, Edinburgh Medical School, Edinburgh, UK

³Beijing Tiantan Hospital affiliated to Capital Medical University, Beijing, China

⁴Institute of Cardiovascular and Medical Sciences, University of Glasgow, Glasgow, UK

⁵Centre for Cognitive Ageing and Cognitive Epidemiology, University of Edinburgh, Edinburgh, UK

Word Count:

Abstract – 348

Main text – 4537

References – 50

Abstract:

Background

Cerebral small vessel disease (SVD) is a major cause of stroke and dementia. The underlying cerebrovascular dysfunction is poorly understood. We investigated cerebrovascular reactivity, blood flow, vascular and cerebrospinal fluid (CSF) pulsatility, and their independent relationship to SVD features, in patients with minor ischaemic stroke and MRI evidence of SVD.

Methods

We recruited patients with minor ischaemic stroke and assessed CVR using Blood Oxygen Level Dependent (BOLD) MRI during a hypercapnic challenge, cerebral blood flow, vascular and CSF pulsatility using phase contrast MRI, and structural MR brain imaging to quantify white matter hyperintensities (WMH) and perivascular spaces (PVS). We quantified CVR in seven white matter and six subcortical grey matter regions, measured blood flow in carotid and vertebral arteries, intracranial venous sinuses, internal jugular veins and CSF flow at the aqueduct and foramen magnum. We used multiple regression to identify SVD features, blood flow and pulsatility parameters associated with CVR, controlling for patient characteristics.

Results

In 53 of 60 patients with complete data (age 68.0 ± 8.8 , 74% male, 75% hypertensive), CVR in grey and white matter decreased with increasing blood pressure (BP, respectively $-0.001\%/mmHg$, $p=0.01$ and $-0.006\%/mmHg$, $p=0.01$, per mmHg increase in BP). After controlling for age, gender and systolic BP, white matter CVR decreased with increasing WMH volume ($-0.01\%/mmHg$ per log₁₀ increase in WMH volume, $p=0.02$) and basal ganglia PVS ($-0.01\%/mmHg$ per point increase in PVS score, $p=0.02$). White matter CVR decreased with increasing venous pulsatility (superior sagittal sinus $-0.03\%/mmHg$, $p=0.02$, per unit increase in pulsatility index) but not with cerebral blood flow ($p=0.58$). Lower foramen magnum CSF stroke volume was associated with worse white matter CVR ($0.04\%/mmHg$ per ml increase in stroke volume, $p=0.04$) and increased basal ganglia PVS.

Conclusions

Contemporaneous assessment of CVR, intracranial vascular and CSF pulsatility demonstrates important interrelationships of these vascular functions in humans. Decreased CVR, increased venous pulsatility and reduced foramen magnum CSF stroke volume suggests that dynamic vascular dysfunctions underpin PVS dysfunction and WMH development. Improved understanding of microvascular dysfunction and CSF dynamics offers new intervention targets to reduce SVD lesion development and their impact on cognitive dysfunction and stroke.

Introduction:

Cerebral small vessel disease (SVD) causes lacunar ischaemic stroke, vascular cognitive impairment and dementia, intracerebral haemorrhage and gait and bladder dysfunction with prevalence increasing with age.(1) Diagnosis is via acute presentation with a lacunar stroke syndrome, cognitive dysfunction or mobility problems, and with neuroimaging findings such as a recent small subcortical infarct, white matter hyperintensities (WMH), lacunes or microbleeds.(2)

There is no specific treatment for SVD as yet.(3) An improved understanding of disease mechanisms is required to identify drug targets. The role of cerebral blood flow (CBF) in SVD is complex: whilst lower CBF is associated with more severe SVD in cross-sectional studies, most longitudinal studies have not found lower CBF to precede development or progression of SVD,(4) and dynamic measures of CBF may be more sensitive to small vessel dysfunction. Reliable measures of vascular function would help screen potential treatments in early phase trials(5) prior to definitive but costly trials with clinical endpoints that require large sample sizes and long follow up periods.(6) Sensitive measures of early cerebrovascular dysfunction might also help personalise therapies.

Cerebrovascular reactivity (CVR) measures the ability of cerebral blood vessels to increase CBF in response to metabolic demands.(7) CVR can be assessed by measuring blood flow changes in response to a vasoactive stimulus such as increased carbon dioxide in inspired air, breath holding, or acetazolamide injection.(8) Transcranial Doppler (TCD) ultrasound is commonly used but only measures large basal cerebral arteries and lacks spatial resolution.(9, 10) Magnetic resonance imaging (MRI) techniques measure CVR in all brain tissues, including the subcortical areas commonly affected by SVD.(11) So far, MRI-based CVR has been assessed in relatively few small studies in SVD, but used different CVR challenges,(12-16) and did not account for clinically-relevant variables (e.g. age, blood pressure [BP], gender) that could confound CVR associations with SVD features.(12)

Vascular pulsatility measured outside the brain is associated with increasing WMH(17, 18) consistent with the hypothesis that SVD is associated with increased arterial stiffening. Also, middle cerebral artery (MCA) pulsatility increases with increasing WMH on TCD,(9, 10) but TCD cannot measure intracranial veins, venous sinuses, or cerebrospinal fluid (CSF) pulsatility, precluding a complete assessment of intracranial pulsatility across key fluid compartments. MRI with phase contrast angiography can assess pulsatility and flow in the intracranial arteries, veins, venous sinuses and CSF spaces (e.g. aqueduct, foramen magnum) within one examination, concurrently with CVR, making it possible to assess relationships between CVR, CBF and pulsatility directly. However, there are very few studies of intracranial pulsatility assessed with MRI in ageing or SVD(19) and no studies in humans of CVR assessed concurrently with intracranial vascular pulsatility, CSF flow dynamics, or resting CBF, to provide a complete assessment of intracranial haemodynamics.

We aimed to assess CVR and patient demographic variables, vascular risk factors and imaging features of SVD, concurrently with total CBF, arterial, venous and CSF pulsatility. We studied independent patients with a past history of minor ischaemic stroke stratified by SVD burden as representative of a high risk group for the clinical effects of SVD. We hypothesised that more severe SVD features on neuroimaging would be associated with reduced CVR, that reduced CVR would associate with increased vascular pulsatility, and that these relationships would persist after controlling for patient demographic and vascular risk factors.

Methods:

Patients

We recruited patients presenting to our regional stroke service between October 2014 and April 2016 with symptomatic non-disabling ischaemic stroke (Modified Rankin score ≤ 3). We also invited such patients who had participated in recent previous prospective studies.(20) All patients had a clinical stroke diagnosis confirmed by a specialist stroke physician and brain imaging that either confirmed a relevant recent infarct or, if no recent infarct was visible, excluded any other cause of the presenting symptoms.(20)

We excluded patients who were pregnant, unable to lie flat, had contraindications to MRI (including claustrophobia), moderate to severe chronic respiratory disease or symptomatic cardiac failure, personal history or first degree relative with subarachnoid haemorrhage or intracranial aneurysm, uncontrolled hypertension, or atrial fibrillation with fast ventricular response.

All participants provided written informed consent prior to enrolment. The study was approved by the UK Health Research Authority National Research Ethics Service Committee East Midlands, Nottingham 1 (ref. 14/EM/1126).

We performed the study assessments at least one month after the patient's stroke to prevent haemodynamic changes in the acute phase of stroke (both stroke related and due to commencing vasoactive secondary prevention medications) from interfering with the interpretation of vascular function. We requested participants not to consume caffeinated drinks on the day of assessment.

We recorded detailed medical histories including clinical characteristics of presenting stroke, vascular risk factors, concurrent medications, and investigations performed for the presenting stroke (diagnostic brain MRI, carotid ultrasound imaging, haematology, biochemistry, electrocardiograms).

We classified the clinical stroke syndrome according to the Oxford Community Stroke Project classification(21) (independently assessed by two stroke physicians, FD and GB) and the lesion type seen on imaging (independently assessed by JMW and YS). Where no recent ischaemic lesion was evident, the final stroke type was assigned using the clinical classification. Where the imaging lesion was discordant with the clinical stroke type, the imaging type was used as the final classification, as previously.(22)

We recorded blood pressure (BP) seven times at standard time points before, during and after MRI.

MRI

We performed brain MRI using a 1.5 Tesla GE research MRI scanner (Signa H Dxt, General Electric, Milwaukee, WI) operating in research mode and an 8-channel phased array head coil. Total imaging time was circa 75 minutes for each participant, but patients were allowed to move and have a natural break between each section of scans to ensure they remained comfortable. We acquired 3D T1-weighted, axial T2-weighted, fluid attenuated inversion recovery (FLAIR) and gradient echo sequences. We performed BOLD MRI scanning with CO₂ challenge at 4mm isotropic resolution acquiring a whole brain volume every three seconds.(11) We performed phase contrast MRI to measure pulsatility in the internal carotid arteries, intracranial venous sinuses, CSF flow (aqueduct, foramen magnum) and total CBF, as described in detail.(23) Full parameters of all MR sequences are in Supplementary Table 1.

The CVR method used BOLD 2-dimensional echo-planar imaging with a CO₂ challenge (detailed in(11)). Briefly, during MRI, patients wore an anaesthetic face mask, carefully fitted to avoid gas leak between mask and face, attached to a bespoke unidirectional breathing circuit (Intersurgical, Wokingham, UK). Monitoring equipment recorded pulse rate, oxygen saturation, BP (Millennia 3155A and Magnitude 3150 MRI; Invivo, Best, The Netherlands) and end-tidal CO₂ (EtCO₂; CD3-A AEI Technologies, Pittsburgh, USA) throughout the examination. During a 12-minute BOLD MRI scan, patients breathed medical air and 6% CO₂ in air (BOC Special Products, UK) alternately, delivered as two minutes air, three minutes CO₂, two minutes air, three minutes CO₂, finishing with two minutes air. We instructed patients to expect a change in smell and breathing pattern (deeper, faster or more forceful breathing), then each patient tried the facemask and gasses before entering the scanner room. Patients were instructed to breathe normally and to press a buzzer to stop the scan if required. Scanning commenced when the patient was fully positioned in the scanner bore, indicated they felt comfortable, and blood pressure and heart rate readings indicated no sign of anxiety or distress. A physician monitored the patient during CO₂ inhalation.

Arterial and venous flow waveforms were measured as described previously.(23-25) Briefly, we used a 2D cine phase-contrast sequence with retrospective peripheral pulse gating to acquire 32 velocity images per cardiac cycle. We used the following slice locations to measure flow in the different structures: a slice superior to the carotid bifurcation and perpendicular to the internal carotid artery (ICA) walls to measure flow in the ICA, vertebral arteries (VA) and internal jugular veins (IJV); a coronal-oblique slice intersecting the superior sagittal sinus approximately 2cm above the torcular and through the midpoint of the straight sinus to measure superior sagittal sinus (SSS), straight sinus (StS) and transverse sinus (TS) flow; a slice perpendicular to the aqueduct for aqueduct CSF flow and an axial slice at the cranio-cervical junction for foramen magnum CSF flow.

Image Processing and Analysis

Investigators were blinded to patient clinical data, CVR, pulsatility and CBF results for all analysis.

Structural image analysis of SVD features was performed according to the STRIVE criteria(2) under the supervision of an expert neuroradiologist (JMW).

We (YS, JMW) scored the following features: WMH using the Fazekas scale, summing periventricular and deep WMH scores to give a score from 0-6; perivascular spaces (PVS), scored separately in the basal ganglia and centrum semiovale, using a validated, semi-quantitative ordinal scale (range 0-4); lacunes (location, number); and microbleeds (BOMBS scale) presence/absence and total number(2); and total SVD score (0-4) by combining WMH, lacunes, microbleeds and PVS scores as described previously.(26)

We co-registered each subject's structural images. We calculated WMH volumes using a validated semi-quantitative technique described previously.(23) Briefly we generated WMH probability maps for each subject using FLAIR and T1W image data. Hyperintense outliers within the white matter surface were defined as voxels with a z score ≥ 1.5 on FLAIR to create an initial estimate of WMH volume. We produced final estimates using 3D smoothing to account for partial volume effects and reduce noise, before manually removing the index and any prior stroke lesions. We segmented normal appearing tissues (cortical grey matter, subcortical grey matter, white matter, cerebellum) and whole brain volume from each subject's T1W data and local population specific probability maps.(27) We calculated intracranial volumes using a semi-automatic method based on T2*W images. All tissue masks were visually inspected and manually corrected as necessary.

We processed CVR images as described previously.(11) We generated voxel-wise CVR maps by regressing the BOLD signal against EtCO₂ and the BOLD scan number (to account for signal drift). CVR is expressed as % BOLD signal change/mmHg change in EtCO₂, based on the EtCO₂ regressor in the model. We made additional adjustment for the delay time between BOLD signal change and EtCO₂ change to minimise the residual sum of squares individually for each voxel, further adjusted by 4 seconds to account for the delay between exhalation and detection on the EtCO₂ monitor caused by the eight metre sample line.

We realigned BOLD images (using SPM 8, <https://www.fil.ion.ucl.ac.uk/spm/software/spm8/>) prior to determining the transformation between BOLD and T2W image spaces (using FSL FLIRT(28)). We then manually drew three subcortical grey matter (thalamus, putamen, caudate head) and four subcortical white matter (frontal, posterior, periventricular and centrum semiovale) regions of interest (ROI) on T1W images before transfer to the BOLD images. Voxels that were part of large vessels or the patient's stroke lesion were manually excluded. We extracted the mean signal across the ROI and fitted the CVR model to that data. We also averaged all grey and white matter regions to give a combined deep grey matter and white matter CVR value.

To process the phase contrast data we drew manual ROI's around right and left ICAs and VAs, the sagittal, straight, right and left transverse sinuses and internal jugular veins, the aqueduct and the foramen magnum subarachnoid space. Background ROIs were placed close to the ROI's to correct background phase error by subtracting the background velocity ('noise') from the ROI velocity. We calculated sum flow and mean velocity for bilateral structures, then total CBF as the sum of ICA and VA flow, normalised to total brain volume and expressed as ml/min/100ml brain tissue. Pulsatility index (PI) in each structure was calculated as $(Flow_{\text{maximum}} - Flow_{\text{minimum}})/Flow_{\text{mean}}$; Resistivity index (RI) was calculated as $(Flow_{\text{maximum}} - Flow_{\text{minimum}})/Flow_{\text{maximum}}$. The reproducibility of this approach is published.(23)

Statistical Analysis

We performed statistical analyses using R version 3.3.0 (<https://cran.r-project.org/>) and the additional packages Hmisc, texreg, data.table, htmlTable, car and psych. We assessed distribution of all variables prior to analysis and log transformed the WMH volumes and atrophy scores due to a skewed distribution. The BP values presented are means of the seven readings taken across the visit. We assessed the relation of demographic factors, SVD features, pulsatility and CBF parameters to CVR values using univariate and then multiple linear regression, adjusting for age, systolic BP and gender, based on those factors identified in our systematic review as potentially influencing CVR,(12) (univariate associations are presented only for completeness). Additionally we adjusted for WMH volume in some models to assess if relationships were independent of a co-association, since we found previously that failure to control for WMH was a potential confound in assessments of CVR in patients with SVD.(6) We examined the normality of residuals (QQ plots and histograms) and heteroscedascity (residual versus fitted values) to assess modelling assumptions. We checked variable inflation factors to assess for collinearity between variables, with a limit of two applied.(29)

Results:

Study Population

We recruited 60 patients; 53 subjects completed the full CVR scanning protocol with complete and fully analysable data. Three withdrew due to claustrophobia when wearing the facemask in the MRI scanner, in one movement artefact precluded analysis, two failed to show any EtCO₂ or BOLD signal change with CO₂ (likely due to a poor fitting mask), and in one patient the acquisition was stopped after initial structural scanning showed an incidental asymptomatic subdural haematoma.

The cohort had a mean age of 68.0±8.8 years (range 52-88 years), 39 (73%) were male. Median NIHSS at presentation with stroke was 2 (range 0-5). At the time of CVR scanning, 75% had hypertension, 66% had hyperlipidaemia, 13% had diabetes, 30% were current smokers or had stopped within the past 12 months and 19% consumed alcohol regularly in excess of recommended limits (table 1). Subjects were scanned at a median of 92 days post stroke (range 32-1768 days).

Imaging features of SVD were common: 27 patients (51%) had deep Fazekas score ≥2 and 29 (55%) had periventricular Fazekas ≥2 indicating moderate to severe WMH; 17 (32%) had basal ganglia PVS score ≥3 and 28 (53%) had centrum semiovale PVS score ≥3 indicating high PVS visibility; 35 (66%) had lacunes; and four patients (8%) had microbleeds.

Univariate Analysis

CVR and Patient characteristics

Higher systolic BP and pulse pressures were associated with reduced CVR in white matter (all p=0.01) and grey matter (all p=0.01; Supplementary Table 2). Reduction of white matter CVR with increasing age did not reach statistical significance (p=0.09). We found no other statistically significant associations with reduced CVR.

CVR and SVD Features

Numerous SVD features were associated with lower white matter CVR (Figure 1, Supplementary Table 2): increased WMH volume, worse WMH Fazekas scores, more PVS, presence of lacunes, deep atrophy and total SVD score (all p<0.05). Reduced grey matter CVR was only associated with periventricular WMH Fazekas score and basal ganglia PVS (both p<0.05).

CVR, Pulsatility and CBF

Reduced white matter CVR was associated with increased PI and RI in the superior sagittal, straight and transverse sinuses (all p<0.05), but not with ICA or internal jugular vein PI or RI, or with CBF, (Figure 2, Supplementary Table 2).

We found no univariate associations between CSF pulsatility or flow measures and CVR.

Co-variate-adjusted analyses

CVR and SVD Features

After controlling for age, systolic BP and gender, we found reduced white matter CVR remained associated with WMH volume (-0.01 %/mmHg change in EtCO₂ per log₁₀ increase in WMH volume, p=0.02), periventricular WMH Fazekas score (-0.01 %/mmHg change in EtCO₂ per point increase, p=0.02) and basal ganglia PVS score (-0.01 %/mmHg change in EtCO₂ per point increase, p=0.02). The associations between these SVD features and grey matter CVR was no longer significant (Table 2). We saw a similar pattern when pulse pressure was substituted for systolic BP (data not shown).

Deep and total Fazekas scores, centrum semiovale PVS, lacunes, any brain atrophy, and total SVD score were not associated with reduced CVR in either white or grey matter (Table 2).

We tested the independence of the basal ganglia PVS score association with reduced white matter CVR further by adding WMH volume to the regression model, which resulted in the association no longer being significant (Supplementary Table 3).

CVR, Pulsatility and CBF

After correcting for age, SBP and gender, reduced white matter CVR remained associated with increasing superior sagittal sinus PI (-0.03 %/mmHg change in EtCO₂ per unit increase in PI p=0.02), superior sagittal sinus RI (-0.07%/mmHg change in EtCO₂ per unit increase in RI, p=0.03), and internal jugular vein PI (-0.01%/mmHg change in EtCO₂ per unit increase in PI, p=0.04), Table 3.

Reduced white matter CVR was also associated with reduced CSF stroke volume at the foramen magnum (-0.04%/mmHg change in EtCO₂ per ml decrease in CSF stroke volume, p=0.04). Furthermore, reduced CSF stroke volume was associated with increased basal ganglia PVS score (-0.96ml per point increase in PVS score, p=0.09, Supplementary Table 4). We saw a similar pattern when pulse pressure was substituted for systolic BP (data not shown).

There was no association of white or grey matter CVR with arterial PI or RI, or with CBF (Table 3).

We further tested the association of superior sagittal sinus and internal jugular vein pulsatility metrics by adding WMH volume into the regression model. Internal jugular vein (but not SSS) PI remained associated with reduced white matter CVR (-0.01%/mmHg change in EtCO₂ per unit increase in PI, p<0.05, Supplementary Table 3).

Discussion:

We measured concurrently several indices of intracranial microvascular function in patients with minor ischaemic stroke and features of SVD on neuroimaging. We demonstrate that reduced CVR is associated with increased WMH burden and increased basal ganglia PVS, independently of age, gender and blood pressure. The association was stronger for white matter than for subcortical grey matter CVR. Furthermore, the association between reduced CVR and WMH was stronger for periventricular than deep WMH, perhaps reflecting more periventricular vulnerability to haemodynamic changes at distal end arteries, or differing pathogeneses of WMH by brain region, providing *in vivo* support in humans for two longstanding hypotheses. We also demonstrated that reduction in white matter CVR was associated with increased intracranial vascular pulsatility, most clearly seen in the intracranial venous sinuses and internal jugular veins, and with increased PVS visibility.(23) Importantly, we also found that reduced CVR was associated with reduced CSF stroke volume at the foramen magnum, and also that reduced CSF stroke volume was associated with increased basal ganglia PVS, showing for the first time in the intact human cranium, a possible link between dysfunctional brain interstitial fluid drainage (evidenced by increased PVS visibility) and impaired CSF pulsation (thought to help flush interstitial fluid through the glymphatic system).(30) We saw no association of reduced CVR in white or grey matter with resting CBF, or of resting CBF with any measures of SVD.

We recruited patients representative of the range of SVD features present in patients with typical lacunar or minor cortical ischaemic stroke to ensure relevance to patients that are commonly affected by SVD.(31, 32) Confirming that vascular function changes in SVD are not confined to one stroke type increases the generalisability of our findings. Stroke type and SVD imaging features were carefully assessed by experienced specialists using standardised, validated image processing and analysis techniques. CVR was measured by a robust and standardised technique with quantified reliability and reproducibility.(11) We were careful to control the statistical analyses for key patient characteristics and WMH volume where appropriate, all guided by a professional statistician.

There are limitations. Whilst this study is one of the largest in the literature to assess CVR in SVD(12) and the only study so far in humans to assess CVR, vascular and CSF pulsatility and CBF simultaneously, the sample size limits the number of comparisons and adjustment variables. We used a 1.5T MRI scanner, however the main impact of this versus a 3T scanner is less 'crisp' structural resolution of the BOLD MRI image which may affect the precision of tissue localisation, but not signal magnitude.(33) However, since we registered all the images into a common image processing space and used ROIs obtained from high quality structural images mapped onto the CVR image to extract the tissue-specific CVR signals, the 1.5T MRI is unlikely to have affected the tissue associations.

We found a strong association of reduced CVR with WMH visual score and volume. However, the Fazekas score allowed us to detect the novel finding of a stronger association between reduced CVR and periventricular than deep WMH. This could reflect reduced vascularity of the distal perforating arterioles and is consistent with recent findings in two similar populations where reduced retinal arteriolar branching complexity (the retina being a surrogate for brain microvessels) was associated with WMH and other SVD features.(34) The finding of a stronger association between reduced CVR and periventricular rather than deep WMH should be replicated in future studies which should examine regional WMH rather than just total volume, since we show that total volume may obscure important differences in relationships between SVD lesions and microvascular function.

Previous studies found various associations between CVR and WMH in different populations. Yezhuvath et al (n=25) found reduced CVR with increasing WMH volume in Alzheimer's disease.(35) Hund-Georgiadis et al (n=17) found reduced CVR in association with a composite SVD severity score including WMH in patients with stroke.(36) Uh et al (n=33) found that CVR in normal white matter declined with increasing WMH volume in older participants with WMH.(37) Van Opstal et al. (n=60) demonstrated BOLD reactivity in the occipital cortex is reduced in individuals with symptomatic hereditary cerebral amyloid angiopathy who had severe WMH and microbleeds compared to controls and presymptomatic carriers.(38)

In several papers by Sam et al. a cohort of patients (n=45-75) over 50 years of age with WMH of Fazekas grade 2 or more, presenting to a neurology clinic with a wide variety of symptoms, demonstrated several associations with altered CVR. Areas of normal white matter with both lower and delayed CVR progressed to become WMH(13, 15) and areas with negative CVR (reduced blood flow below baseline during CO₂ inhalation, possibly suggestive of a vascular steal phenomenon) were associated with lower CBF and microstructural damage on DTI.(14) Lower CVR, FA, CBF and increased T2 and MD were observed in WMH compared with contralateral normal white matter.(16)

In contrast, three studies did not show associations between CVR and WMH, although WMH burden was low in all three. Gauthier et al (n=85) found no association of WMH volume with CVR, however the mean WMH volume in their cohort was small (1.0±1.7ml)(39) and they did find CVR in periventricular watershed areas to be positively associated with general fitness assessed as maximum aerobic capacity (VO₂ max).(39) Richiardi et al. (n=63) found no association between their unique "CVR velocity" metric and Fazekas score in patients with Alzheimer's disease or mild cognitive impairment or healthy older subjects(40) but the WMH burden was low and their CVR velocity method is very different to that used here and in most prior studies (CO₂ delivery via nasal cannulae and no monitoring of EtCO₂). Conijn et al. (n=49) found no association of CVR and WMH volume in younger subjects with few WMH.(41)

Our systematic review highlighted the variability of CVR associations with regard to patient characteristics.(12) The association of reduced CVR with increased BP was seen in some prior studies (41, 42) but BP associations with CVR were unclear in many other studies. A trend for increasing age to be associated with reduced CVR narrowly failed to reach significance in our study, but age was associated with reduced CVR in several other studies.(36, 39, 41, 43) The lack of a definite age-CVR relationship in the present study may reflect poorer brain vascular health in the younger compared with the older stroke patients since patients who experience a stroke aged in their 40s or 50s may have worse vascular health than those who do not experience stroke until their ninth decade. This paradox has almost certainly dampened the expected age effect.

Reduced CVR may be associated with other markers of vascular health and symptoms. Reduced CVR was associated with raised inflammatory markers(44) and more rapid decline in gait speed in diabetics(45) and with decreased insulin sensitivity in obese individuals with insulin resistance.(46) The literature on CVR and cognitive performance is inconclusive.(47)

We are the first to describe an association of increased PVS with reduced CVR and CSF stroke volume, in addition to increased intracranial vascular pulsatility.(23) Visible PVS are associated with hypertension, increasing age, systemic and intracerebral inflammation, other SVD features like WMH and microbleeds, and increased risk of dementia.(1) Longitudinal studies are required to demonstrate if PVS visibility precedes or follows impairments in CVR or changes in vascular or CSF pulsatility. PVS are part of the brain's waste clearance and immune defence system, recently referred to as the glymphatic system;(48) in this regard, it is interesting that we detected altered

pulsation of the CSF at the foramen magnum in association with reduced CVR and with worse PVS since, in experimental models, reduced PVS flushing may lead to failed clearance of metabolic debris and PVS dilation.(30, 48) CSF stroke volume at the foramen magnum was recently shown to be related to inspiration and improved venous return(49)– we extend this work by demonstrating relationships between CSF stroke volume and increased PVS visibility. Reduced CSF stroke volume could indicate reduced CSF flux around the base of the brain with reduced CSF movement linked to impaired PVS flushing. Caution is required, however, since the PVS-CSF stroke volume and CVR associations could be a co-association with other SVD features, a common problem in SVD research(6) and should be evaluated further.

We did not find an association between WMH and CBF, consistent with prior data.(4) However, we provide more support for a vascular dysfunction in SVD: CVR is a measure of dynamic vessel function, with impairment reflecting an inability to increase blood flow when required. The mechanisms behind this may encompass impaired endothelial function, reduced nitric oxide bioavailability, altered vascular smooth muscle function, inflammatory exudates damaging the vessel wall and perivascular space function.(50) More longitudinal data with contemporaneous vascular function measures and careful adjustment for co-variables are required to unpick this pathway, but it is notable that all the associations of demographic and SVD features with impaired CVR were stronger in the white matter than the grey matter despite white matter CVR being around one third the magnitude of that in grey matter and white matter CBF being around half of that in grey matter.(4, 23) Studies of SVD mechanisms and potential interventions should consider using measures of dynamic vascular function such as CVR or pulsatility rather than resting CBF.(5, 38)

Conclusions and future directions

We show novel and independent associations between SVD features and several measures of impaired cerebral haemodynamics, providing new insights into mechanisms that may underlie SVD development. Further longitudinal studies, controlling for confounders (age, BP, WMH volume, etc) will define these changes and delineate the pathway of SVD development, including the novel observation of impaired CSF pulsation. Ultimately, enhanced knowledge of vascular malfunction will help identify therapeutic targets to halt or even reverse disease progression, with benefits for both dementia and stroke prevention.

Funding:

Funding for the study was provided by the Chief Scientist Office (Scotland), grant reference ETM/326 and the Wellcome Trust – University of Edinburgh Institutional Strategic Support Fund. Additional support is provided by the European Union Horizon 2020 project No. 666881, ‘SVDs@Target’ (GWB, MS), The Stroke Association Princess Margaret Research Development Fellowship scheme (GWB), Alzheimer’s Society (Ref: 252(AS-PG-14-033), GWB), the Stroke Association Garfield Weston Foundation Senior Clinical Lectureship (FND), NHS Research Scotland (FND), the Stroke Association Postdoctoral Fellowship (TSAPDF2017/01, DAD), the China Scholarships Council/University of Edinburgh (YS), NHS Lothian Research and Development Office (MJT), the Scottish Funding Council through the Scottish Imaging Network, A Platform for Scientific Excellence (SINAPSE) Collaboration. Funding is gratefully acknowledged from the Fondation Leducq (ref no. 16 CVD 05) and Edinburgh and Lothians Health Foundation.

References

1. DeBette S, Schilling S, Duperron M-G, Larsson SC, Markus HS. Clinical Significance of Magnetic Resonance Imaging Markers of Vascular Brain Injury: A Systematic Review and Meta-analysis. *Clinical Significance of Magnetic Resonance Imaging Markers of Vascular Brain Injury*. *JAMA Neurol.* 2019;76(1):81-94.
2. Wardlaw JM, Smith EE, Biessels GJ, Cordonnier C, Fazekas F, Frayne R, et al. Neuroimaging standards for research into small vessel disease and its contribution to ageing and neurodegeneration: a united approach. *Lancet Neurol.* 2013;12(8):822-38.
3. Bath PM, Wardlaw JM. Pharmacological treatment and prevention of cerebral small vessel disease: a review of potential interventions. *Int J Stroke.* 2015;10:469-78.
4. Shi Y, Thrippleton MJ, Makin SD, Marshall I, Geerlings MI, de Craen AJ, et al. Cerebral blood flow in small vessel disease: A systematic review and meta-analysis. *J Cereb Blood Flow Metab.* 2016;36(10):1653-67.
5. Blair GW, Appleton JP, Flaherty K, Doubal F, Sprigg N, Dooley R, et al. Tolerability, Safety and Intermediary Pharmacological Effects of Cilostazol and Isosorbide Mononitrate, Alone and Combined, in Patients with Lacunar Ischaemic Stroke: The LACunar Intervention-1 (LACI-1) Trial. *Lancet.* 2018; In press.
6. Blair GW, Hernandez MV, Thrippleton MJ, Doubal FN, Wardlaw JM. Advanced Neuroimaging of Cerebral Small Vessel Disease. *Curr Treat Options Cardiovasc Med.* 2017;19(7):56.
7. Blair GW, Doubal FN, Thrippleton MJ, Marshall I, Wardlaw JM. Magnetic resonance imaging for assessment of cerebrovascular reactivity in cerebral small vessel disease: A systematic review. *J Cereb Blood Flow Metab.* 2016;36(5):833-41.
8. Fierstra J, Sobczyk O, Battisti-Charbonney A, Mandell D, Poublanc J, Crawley A, et al. Measuring cerebrovascular reactivity: what stimulus to use? *J Physiol.* 2013;591(23):5809-21.
9. Stevenson SF, Doubal FN, Shuler K, Wardlaw JM. A systematic review of dynamic cerebral and peripheral endothelial function in lacunar stroke versus controls. *Stroke.* 2010;41:e434-e42.
10. Webb AJ, Simoni M, Mazzucco S, Kuker W, Schulz U, Rothwell PM. Increased cerebral arterial pulsatility in patients with leukoaraiosis: arterial stiffness enhances transmission of aortic pulsatility. *Stroke.* 2012;43(10):2631-6.
11. Thrippleton MJ, Shi Y, Blair G, Hamilton I, Waiter G, Schwarzbauer C, et al. Cerebrovascular reactivity measurement in cerebral small vessel disease: Rationale and reproducibility of a protocol for MRI acquisition and image processing. *Int J Stroke.* 2018;13(2):195-206.
12. Blair G, Doubal FN, Thrippleton MJ, Marshall I, Wardlaw JM. Magnetic resonance imaging for assessment of cerebrovascular reactivity in cerebral small vessel disease. A systematic review. *J Cereb Blood Flow Metab.* 2016;36(5):833-41.
13. Sam K, Crawley AP, Conklin J, Poublanc J, Sobczyk O, Mandell DM, et al. Development of White Matter Hyperintensity Is Preceded by Reduced Cerebrovascular Reactivity. *Ann Neurol.* 2016;80(2):277-85.
14. Sam K, Peltenburg B, Conklin J, Sobczyk O, Poublanc J, Crawley AP, et al. Cerebrovascular reactivity and white matter integrity. *Neurology.* 2016;87(22):2333-9.
15. Sam K, Conklin J, Holmes KR, Sobczyk O, Poublanc J, Crawley AP, et al. Impaired dynamic cerebrovascular response to hypercapnia predicts development of white matter hyperintensities. *Neuroimage Clin.* 2016;11:796-801.
16. Sam K, Crawley AP, Poublanc J, Conklin J, Sobczyk O, Mandell DM, et al. Vascular Dysfunction in Leukoaraiosis. *AJNR Am J Neuroradiol.* 2016;37(12):2258-64.
17. Aribisala BS, Morris Z, Eadie E, Thomas A, Gow A, Valdes Hernandez MC, et al. Blood pressure, internal carotid artery flow parameters and age-related white matter hyperintensities. *Hypertension.* 2014;63:1011-8.

18. Pase MP, Grima NA, Stough CK, Scholey A, Pipingas A. Cardiovascular disease risk and cerebral blood flow velocity. *Stroke*. 2012;43(10):2803-5.
19. Shi Y, Thrippleton Michael J, Marshall I, Wardlaw JM. Intracranial pulsatility in patients with cerebral small vessel disease: a systematic review. *Clin Sci*. 2018;132(1):157-71.
20. Makin SDJ, Doubal FN, Dennis MS, Wardlaw JM. Clinically confirmed stroke with negative diffusion-weighted imaging magnetic resonance imaging. Longitudinal study of clinical outcomes, stroke recurrence, and systematic review. *Stroke*. 2015;46:3142-8.
21. Bamford J, Sandercock P, Dennis M, Burn J, Warlow C. Classification and natural history of clinically identifiable subtypes of cerebral infarction. *Lancet*. 1991;337(8756):1521-6.
22. Jackson CA, Hutchison A, Dennis MS, Wardlaw JM, Lewis SC, Sudlow CL. Differences between ischemic stroke subtypes in vascular outcomes support a distinct lacunar ischemic stroke arteriopathy. A prospective, hospital-based study. *Stroke*. 2009;40:3679-84.
23. Shi Y, Thrippleton MJ, Blair GW, Dickie DA, Marshall I, Hamilton I, et al. Small vessel disease is associated with altered cerebrovascular pulsatility but not resting cerebral blood flow. *J Cereb Blood Flow Metab*. 2018;0(0):0271678X18803956.
24. Stoquart-ElSankari S, Baledent O, Gondry-Jouet C, Makki M, Godefroy O, Meyer ME. Aging effects on cerebral blood and cerebrospinal fluid flows. *J Cereb Blood Flow Metab*. 2007;27(9):1563-72.
25. Stoquart-ElSankari S, Lehmann P, Villette A, Czosnyka M, Meyer M-E, Deramond H, et al. A Phase-Contrast MRI Study of Physiologic Cerebral Venous Flow. *J Cereb Blood Flow Metab*. 2009;29(6):1208-15.
26. Staals J, Makin SDJ, Doubal F, Dennis M, Wardlaw JM. Stroke subtype, vascular risk factors and total MRI brain small vessel disease burden. *Neurology*. 2014;83:1228-34.
27. Valdes Hernandez MC, Ferguson KJ, Chappell FM, Wardlaw JM. New multispectral MRI data fusion technique for white matter lesion segmentation: method and comparison with thresholding in FLAIR images. *Eur Radiol*. 2010;20(7):1684-91.
28. Jenkinson M, Bannister P, Brady M, Smith S. Improved optimization for the robust and accurate linear registration and motion correction of brain images. *Neuroimage*. 2002;17(2):825-41.
29. Zuur AF, Ieno EN, Elphick CS. A protocol for data exploration to avoid common statistical problems. *Methods Ecol Evol*. 2010;1(1):3-14.
30. Mestre H, Tithof J, Du T, Song W, Peng W, Sweeney AM, et al. Flow of cerebrospinal fluid is driven by arterial pulsations and is reduced in hypertension. *Nat Commun*. 2018;9(1):4878.
31. Loos CM, McHutchison C, Cvoro V, Makin SD, Staals J, Chappell F, et al. The relation between total cerebral small vessel disease burden and gait impairment in patients with minor stroke. *Int J Stroke*. 2018;13(5):518-24.
32. Wardlaw JM, Makin SJ, Hernández MCV, Armitage PA, Heye AK, Chappell FM, et al. Blood-brain barrier failure as a core mechanism in cerebral small vessel disease and dementia: evidence from a cohort study. *Alzheimers Dement*. 2017;13(6):634-43.
33. Stringer M, Blair G, Shi Y, Hamilton I, Marshall I, Doubal F, et al. A comparison of cerebrovascular reactivity at 1.5 and 3T in cerebral small vessel disease patients. *Proc Intl Soc Mag Reson Med*. 2018;26:4818.
34. McGrory S, Ballerini L, Doubal FND, Staals J, Allerhand M, del C. Valdes-Hernandez M, et al. Retinal microvasculature and cerebral small vessel disease in the Lothian Birth Cohort 1936 and Mild Stroke Study. *bioRxiv*. 2018:462507.
35. Yezhuvath US, Uh J, Cheng Y, Martin-Cook K, Weiner M, Diaz-Arrastia R, et al. Forebrain-dominant deficit in cerebrovascular reactivity in Alzheimer's disease. *Neurobiol Aging*. 2012;33(1):75-82.
36. Hund-Georgiadis M, Zysset S, Naganawa S, Norris DG, Yves von Cramon D. Determination of cerebrovascular reactivity by means of fMRI signal changes in cerebral microangiopathy: a correlation with morphological abnormalities. *Cerebrovasc Dis*. 2003;16:158-65.

37. Uh J, Yezhuvath U, Cheng Y, Lu H. In vivo vascular hallmarks of diffuse leukoariosis. *J Magn Reson Imaging*. 2010;32(1):184-90.
38. van Opstal AM, van Rooden S, van Harten T, Ghariq E, Labadie G, Fotiadis P, et al. Cerebrovascular function in presymptomatic and symptomatic individuals with hereditary cerebral amyloid angiopathy: a case-control study. *Lancet Neurol*. 2017;16(2):115-22.
39. Gauthier CJ, Lefort M, Mekary S, Desjardins-Crépeau L, Skimminge A, Iversen P, et al. Hearts and minds: linking vascular rigidity and aerobic fitness with cognitive aging. *Neurobiol Aging*. 2015;36(1):304-14.
40. Richiardi J, Monsch AU, Haas T, Barkhof F, Van de Ville D, Radü EW, et al. Altered cerebrovascular reactivity velocity in mild cognitive impairment and Alzheimer's disease. *Neurobiol Aging*. 2015;36(1):33-41.
41. Conijn MM, Hoogduin JM, van der Graaf Y, Hendrikse J, Luijten PR, Geerlings MI. Microbleeds, lacunar infarcts, white matter lesions and cerebrovascular reactivity - a 7 T study. *Neuroimage*. 2012;59(2):950-6.
42. Haight TJ, Bryan RN, Erus G, Davatzikos C, Jacobs DR, D'esposito M, et al. Vascular risk factors, cerebrovascular reactivity, and the default-mode brain network. *Neuroimage*. 2015;115:7-16.
43. Liu P, Hebrank AC, Rodrigue KM, Kennedy KM, Section J, Park DC, et al. Age-related differences in memory-encoding fMRI responses after accounting for decline in vascular reactivity. *Neuroimage*. 2013;78:415-25.
44. Chung C-C, Pimentel D, Jor'dan AJ, Hao Y, Milberg W, Novak V. Inflammation-associated declines in cerebral vasoreactivity and cognition in type 2 diabetes. *Neurology*. 2015;85(5):450-8.
45. Chung C-C, Pimentel Maldonado DA, Jor'dan AJ, Alfaro FJ, Lioutas V-A, Núñez MZ, et al. Lower cerebral vasoreactivity as a predictor of gait speed decline in type 2 diabetes mellitus. *J Neurol*. 2018;265(10):2267-76.
46. Frosch OH, Yau PL, Osorio RS, Rusinek H, Storey P, Convit A. Insulin resistance among obese middle-aged is associated with decreased cerebrovascular reactivity. *Neurology*. 2017;89(3):249-55.
47. Catchlove SJ, Pipingas A, Hughes ME, Macpherson H. Magnetic resonance imaging for assessment of cerebrovascular reactivity and its relationship to cognition: a systematic review. *BMC Neurosci*. 2018;19(1):21.
48. Rasmussen MK, Mestre H, Nedergaard M. The glymphatic pathway in neurological disorders. *Lancet Neurol*. 2018;17(11):1016-24.
49. Dreha-Kulaczewski S, Joseph AA, Merboldt K-D, Ludwig H-C, Gärtner J, Frahm J. Identification of the upward movement of human CSF in vivo and its relation to the brain venous system. *J Neurosci*. 2017;37(9):2395-402.
50. Shi Y, Wardlaw JM. Update on cerebral small vessel disease: a dynamic whole-brain disease. *Stroke Vasc Neurol*. 2016;1(3):83-92.

Figure 1: White matter CVR and WMH volume, WMH Fazekas score and PVS scores.

Figure 2: Relationship of white matter CVR, subarachnoid CSF stroke volume and superior sagittal sinus pulsatility index

Table 1: Demographic data of participants by SVD score. Continuous variables expressed as mean +/- SD. Categorical variables expressed as n (%).

	SVD Score 0-1 (N=22)	SVD Score 2-4 (N=31)	All Patients (N=53)
Age at Visit	64.05 +/- 7.18	70.87 +/- 8.76	68.04 +/- 8.75
Male	77% (17)	71% (22)	74% (39)
History of TIA	0% (0)	3% (1)	2% (1)
History of Stroke	14% (3)	13% (4)	13% (7)
Diabetes	14% (3)	13% (4)	13% (7)
Hypertension	64% (14)	84% (26)	75% (40)
Antihypertensive Use Pre-Stroke	50% (11)	58% (18)	55% (29)
Atrial Fibrillation	0% (0)	16% (5)	9% (5)
Hyperlipidaemia	64% (14)	68% (21)	66% (35)
Ischaemic Heart Disease	14% (3)	6% (2)	9% (5)
Current or recent smoking history	32% (7)	19% (6)	25% (13)
History of alcohol excess	27% (6)	13% (4)	19% (10)
Alcohol consumption (units per week)	15.91 +/- 23.82	9.06 +/- 10.63	11.91 +/- 17.49
Current antiplatelet use	100% (22)	84% (26)	91% (48)
Current anticoagulant use	0% (0)	16% (5)	9% (5)
Current Statin Use	91% (20)	90% (28)	91% (48)
Systolic Blood Pressure	136.58 +/- 15.08	145.90 +/- 15.56	142.03 +/- 15.91
Diastolic Blood Pressure	78.62 +/- 8.10	80.32 +/- 8.23	79.61 +/- 8.14
Mean Arterial Pressure	97.94 +/- 9.69	102.18 +/- 9.19	100.42 +/- 9.55
Pulse Pressure	57.97 +/-10.76	65.58 +/-13.64	62.42 +/-12.98
White Matter Hyperintensity Volume (ml) Median (IQR)	7.67 (4.51 - 10.76)	22.50 (9.38 - 35.30)	11.93 (6.45 - 27.10)
WMH Volume (% of intracranial volume), median	0.50 (0.29 - 0.77)	1.40 (0.75 - 2.86)	0.81 (0.45 - 1.66)

(IQR)			
Deep Fazekas Score (median)	1	2	2
Periventricular Fazekas Score (median)	1	2	2
Total Fazekas Score (median)	2	4	3
Basal Ganglia PVS Score (median)	1	2	2
Centrum Semiovale PVS Score (median)	2	3	3
Presence of Lacunes	23% (5)	97% (30)	66% (35)
Deep Atrophy Score (median)	2	3	3
Superficial Atrophy Score (median)	3	4	3
Deep Grey Matter CVR (all regions of interest combined)	0.155 +/- 0.073	0.125 +/- 0.051	0.138 +/- 0.062
White Matter CVR (all regions of interest combined)	0.067 +/-0.032	0.049 +/- 0.023	0.056 +/- 0.028
Lacunar Subtype	59% (13)	74% (23)	68% (36)
Total arterial blood flow (ml/minute/100ml brain tissue)	60.86 +/- 10.51	59.62 +/- 8.12	60.14 +/- 9.13

Table 2: CVR association with stroke subtype and SVD imaging markers. All multivariate regression models adjusted for age, sex and systolic blood pressure. Standardised β co-efficient, 95% confidence interval and p value.

	Deep Grey Matter CVR	White Matter CVR	VIF Range
Stroke Type (lacunar vs Cortical)	$\beta = 0.006$ (-0.031, 0.043) $p = 0.73$	$\beta = 0.001$ (-0.015, 0.264) $p = 0.89$	1.07-1.16
WMH Volume (normalised to ICV)	$\beta = -0.021$ (-0.043, 0.000) $p = 0.05$	$\beta = -0.012$ (-0.021, -0.002) $p = 0.02$	1.10-1.58
Periventricular Fazekas Score	$\beta = -0.023$ (-0.047, 0.002) $p = 0.07$	$\beta = -0.013$ (-0.023, -0.002) $p = 0.02$	1.12-1.48
Deep Fazekas Score	$\beta = -0.011$ (-0.033, 0.011) $p = 0.30$	$\beta = -0.005$ (-0.015, 0.005) $p = 0.30$	1.10-1.35
Total Fazekas	$\beta = -0.009$ (-0.021, 0.003) $p = 0.14$	$\beta = -0.005$ (-0.010, 0.001) $p = 0.08$	1.11-1.41
PVS Score – Basal Ganglia	$\beta = -0.019$ (-0.039, 0.001) $p = 0.07$	$\beta = -0.011$ (-0.019, -0.002) $p = 0.02$	1.10-1.41
PVS Score – Centrum semiovale	$\beta = -0.017$ (-0.034, 0.001) $p = 0.06$	$\beta = -0.007$ (-0.014, 0.001) $p = 0.08$	1.11-1.21
Lacunae	$\beta = -0.017$ (-0.056, 0.022) $p = 0.38$	$\beta = -0.010$ (-0.028, 0.007) $p = 0.23$	1.11-1.29
Deep Atrophy	$\beta = -0.011$ (-0.046, 0.024) $p = 0.53$	$\beta = -0.010$ (-0.025, 0.005) $p = 0.20$	1.10-1.33

Superficial Atrophy	$\beta = -0.011$ (-0.054, 0.032) $p = 0.62$	$\beta = -0.006$ (-0.024, 0.013) $p = 0.56$	1.12-1.36
Combined Atrophy	$\beta = -0.012$ (-0.055, 0.030) $p = 0.56$	$\beta = -0.009$ (-0.028, 0.009) $p = 0.32$	1.10-1.40
Brain Parenchymal Volume (normalised to ICV)	$\beta = 0.38$ (-0.175, 0.936) $p = 0.17$	$\beta = 0.010$ (-0.240, 0.259) $p = 0.94$	1.12-1.32
SVD Score (High vs Low)	$\beta = -0.026$ (-0.063, 0.011) $p = 0.17$	$\beta = -0.011$ (-0.028, 0.005) $p = 0.17$	1.14-1.57

WMH = white matter hyperintensity, PVS = perivascular space, ICV = intracranial volume, VIF = variable inflation factor

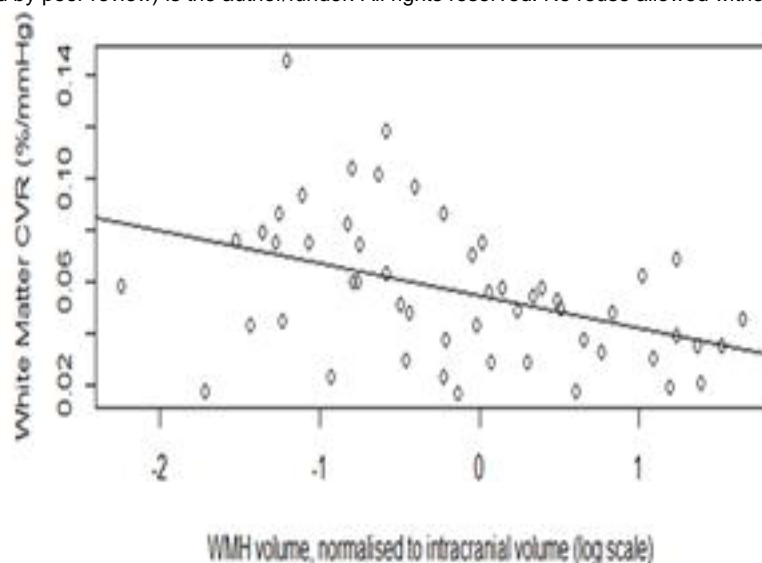
Table 3: CVR association with CBF, arterial and venous pulsatility and CSF flow dynamics. All multivariate regression models adjusted for age, sex and systolic BP. Standardised β co-efficient, 95% confidence interval and p value.

	Deep Grey Matter CVR	White Matter CVR	VIF range
Total cerebral blood flow	$\beta = -0.002$ (-0.004, 0.000) $p = 0.08$	$\beta = 0.000$ (-0.001, 0.001) $p = 0.58$	1.12-1.24
Internal carotid artery PI	$\beta = 0.015$ (-0.046, 0.075) $p = 0.62$	$\beta = 0.003$ (-0.023, 0.030) $p = 0.81$	1.15-1.24
Vertebral artery PI	$\beta = 0.014$ (-0.034, 0.062) $p = 0.56$	$\beta = 0.005$ (-0.017, 0.026) $p = 0.67$	1.10-1.18
Superior sagittal sinus PI	$\beta = -0.040$ (-0.117, 0.037) $p = 0.30$	$\beta = -0.038$ (-0.070, -0.006) $p = 0.02$	1.13-1.21
Straight sinus PI	$\beta = -0.030$ (-0.132, 0.073) $p = 0.56$	$\beta = -0.034$ (-0.078, 0.011) $p = 0.13$	1.14-1.33
Transverse sinus PI	$\beta = -0.052$ (-0.139, 0.034) $p = 0.23$	$\beta = -0.034$ (-0.071, 0.004) $p = 0.08$	1.11-1.26
Internal jugular vein PI	$\beta = -0.025$ (-0.056, 0.006) $p = 0.11$	$\beta = -0.014$ (-0.027, -0.001) $p = 0.04$	1.01-1.13
Internal carotid artery RI	$\beta = 0.027$ (-0.240, 0.294) $p = 0.84$	$\beta = 0.011$ (-0.106, 0.128) $p = 0.85$	1.13-1.31
Vertebral artery RI	$\beta = 0.054$ (-0.163, 0.271) $p = 0.62$	$\beta = 0.013$ (-0.083, 0.108) $p = 0.79$	1.13-1.27
Superior	$\beta = -0.074$	$\beta = -0.070$	1.12-1.20

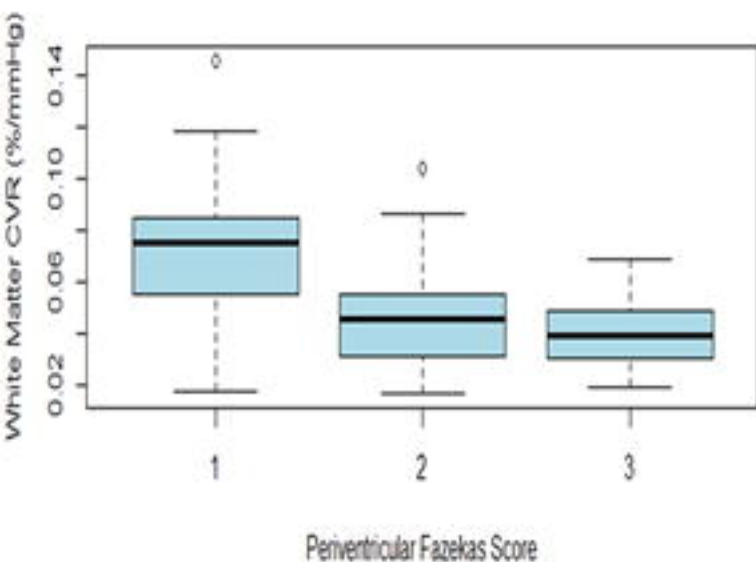
sagittal sinus RI	(-0.219, 0.071) p = 0.31	(-0.131, -0.009) p = 0.03	
Straight sinus RI	$\beta = -0.045$ (-0.224, 0.134) p = 0.62	$\beta = -0.055$ (-0.132, 0.022) p = 0.16	1.13-1.31
Transverse sinus RI	$\beta = -0.077$ (-0.226, 0.073) p = 0.31	$\beta = -0.051$ (-0.116, 0.013) p = 0.12	1.11-1.27
Internal jugular vein RI	$\beta = -0.056$ (-0.136, 0.024) p = 0.16	$\beta = -0.032$ (-0.067, 0.003) p = 0.07	1.01-1.13
Aqueduct CSF flow	$\beta = -0.005$ (-0.029, 0.020) p = 0.71	$\beta = -0.002$ (-0.012, 0.009) p = 0.78	1.07-1.19
Aqueduct CSF stroke volume	$\beta = 0.045$ (-0.213, 0.304) p = 0.73	$\beta = 0.035$ (-0.078, 0.148) p = 0.54	1.13-1.25
Foramen magnum CSF flow	$\beta = 0.001$ (-0.003, 0.005) p = 0.72	$\beta = 0.001$ (-0.001, 0.002) p = 0.51	1.00-1.13
Foramen magnum CSF Stroke Volume	$\beta = 0.003$ (-0.082, 0.087) p = 0.95	$\beta = 0.037$ (0.002, 0.072) p = 0.04	1.01-1.14

PI = Pulsatility Index, RI = Resistivity Index, CSF = cerebrospinal fluid, VIF = variable inflation factor

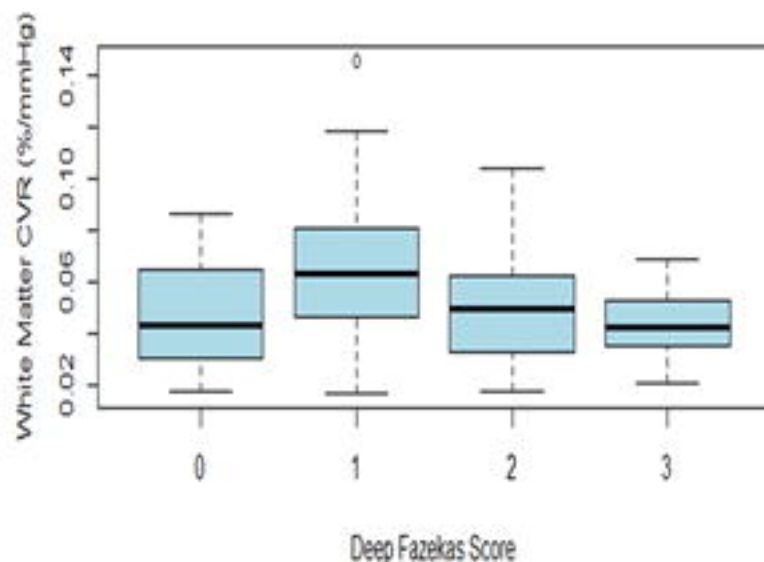
White Matter CVR and WMH Volume



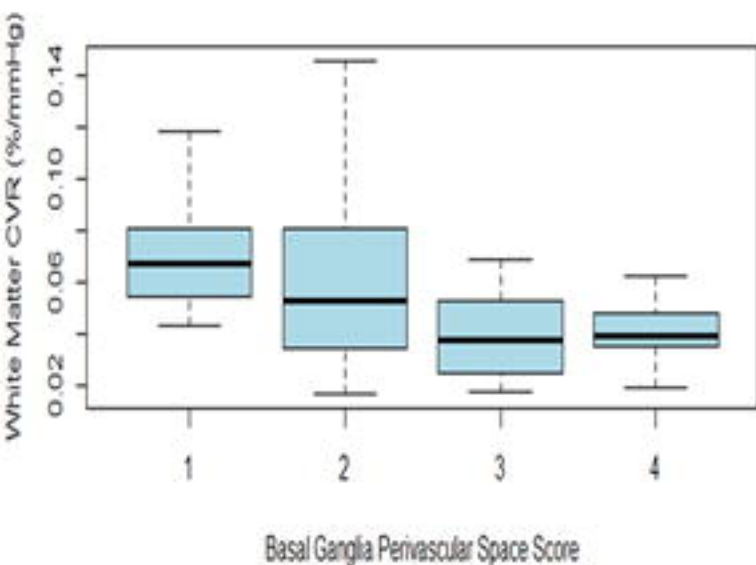
White Matter CVR by Periventricular Fazekas Score



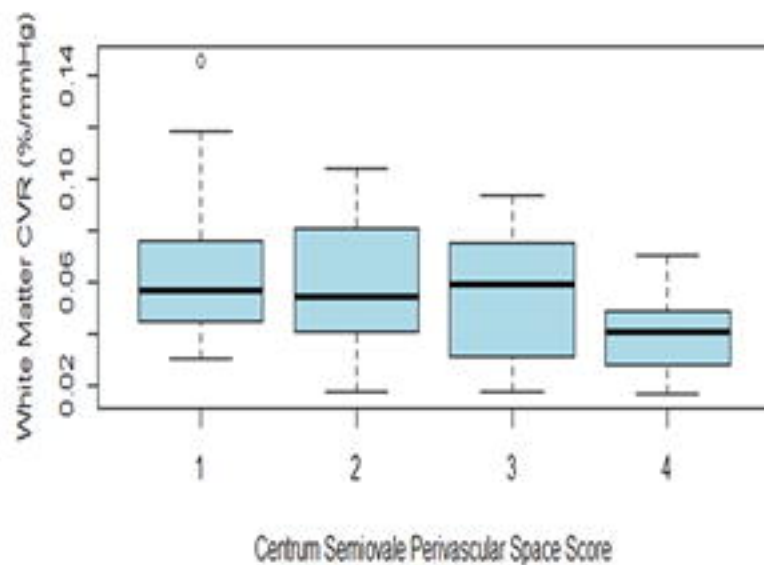
White Matter CVR by Deep Fazekas Score



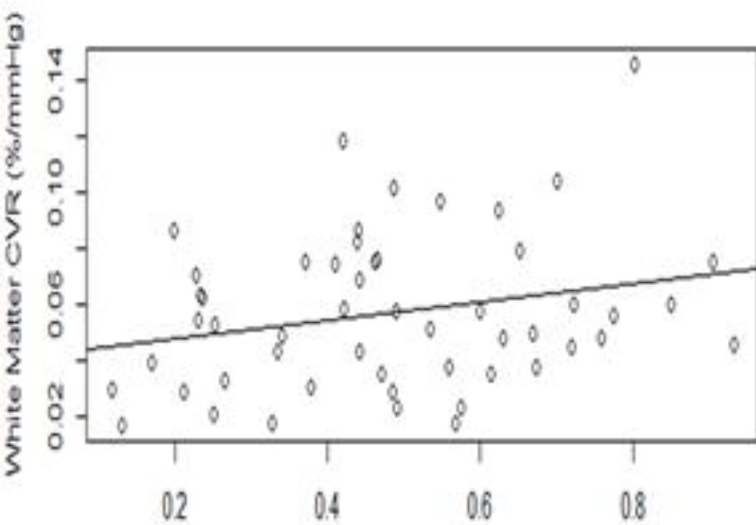
White Matter CVR by Basal Ganglia Perivascular Space Score



White Matter CVR by Centrum Semiovale Perivascular Space Score

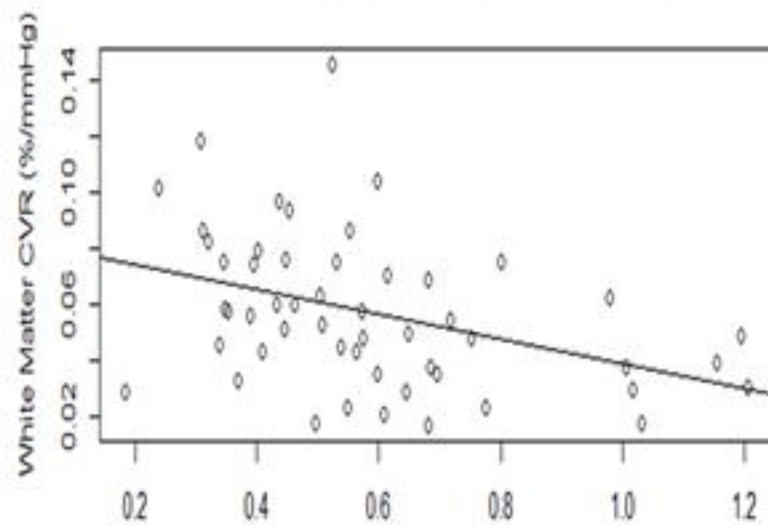


White Matter CVR and Subarachnoid CSF Stroke Volume



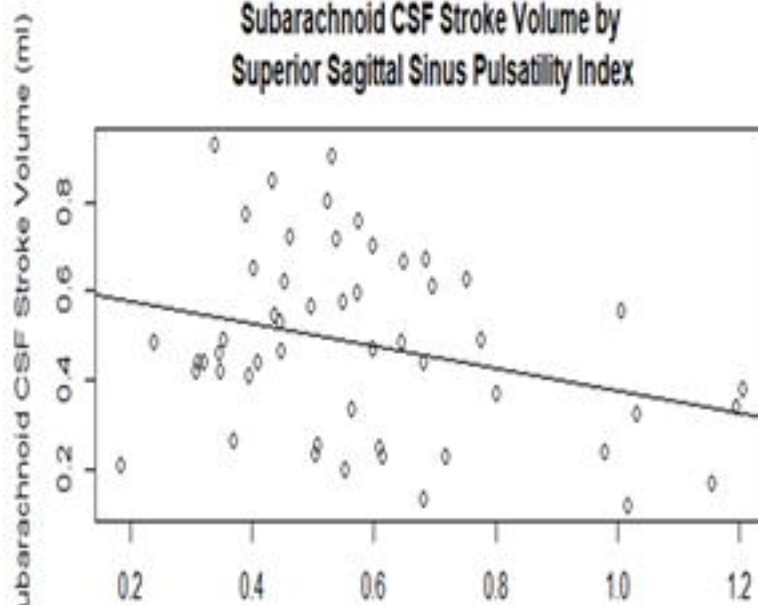
Subarachnoid CSF Stroke Volume (ml)

White Matter CVR by Superior Sagittal Sinus Pulsatility Index



Superior Sagittal Sinus Pulsatility Index

Subarachnoid CSF Stroke Volume by Superior Sagittal Sinus Pulsatility Index



Superior Sagittal Sinus Pulsatility Index